Wireless Energy Transfer Coil System for Industrial Applications

Feng Pan [1], Linfeng Chen [1], Kaikai Cai [1] and V. Singh [1]

[1] Huzhou Juiding Electronics Company, Limited

Abstract. In this paper, a critical component of a wireless charging system that utilizes Near Field Magnetic Coupling (NFMC) is addressed. Specifically, a scalable coil design process is presented that utilizes analytical equations, empirical data, and quasi-static EM simulations. While the coil design can typically be simplified to a transformer with air-core coils and ferrite shielding; the design can become complex under certain use-case conditions. These use-case conditions include spatial flexibility (in the xy plane) at an increased range (z-axis). Using the described process, a three-coil array is designed that can charge a target device up to 5 W at a distance of 30 mm to 40 mm at a frequency range of 100 kHz – 300 kHz, with a projected active charging area of approximately 60 cm^2 (15 cm X 4 cm). The coil-array is scalable in that more coils can be added to increase the active area with minimal impact on the wireless performance.

Keywords: Wireless Charging, Coils, Magnetic Fields, Industrial IoT.

1. Introduction

Wireless Power Transfer (WPT) has become a mainstream application. Applications range from low power systems such as electric toothbrush [1] to high-power applications such as electric vehicle charging [1-2]. Mobile phone wireless charging is also past its critical mass, with over a billion wireless charging-enabled devices in circulation [3]. Other applications include biomedical systems [4] and mobile robots [5].

Many mechanisms are possible for WPT, such as Magnetic Induction/Magnetic Resonance, Radio Frequency, Microwave, Infrared [6-8]. There are tradeoffs in cost, range, efficiency, safety, interference susceptibility and effect from the environment (e.g., dielectric, conductive materials, etc), which has affected the commercial maturity of these technologies.

All Wireless Power systems can simply be represented as a DC-DC converter as shown in Fig. 1 below.

The DC-DC converter encompasses the power conversion (DC-AC) on the transmitting side of the system, the transmitting transducer (antenna, coil, piezoelectric material, array of antennas, etc), the medium (air, dielectric, liquid, human tissue, etc), the receiving transducer and the power conversion (DC-AC) and regulation circuitry on the receiving side of the system.

In this work, the Magnetic Induction/Magnetic Resonance techniques, which are based on the concept of Near Field Magnetic Coupling (NFMC). All NFMC systems can be described at a high level in Fig. 2.
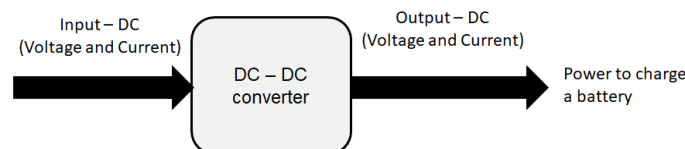

Fig. 1. A generalized representation of all wireless power systems. The DC-DC converter portion includes the power converstion electronics at the transmitting and receiving sides, the antennas and the medium.

This work is concerned with the Magnetic Induction/Magnetic Resonance techniques, which are based on the concept of Near Field Magnetic Coupling (NFMC). All NFMC systems can be described at a high level as the following schematic (Figure 2).
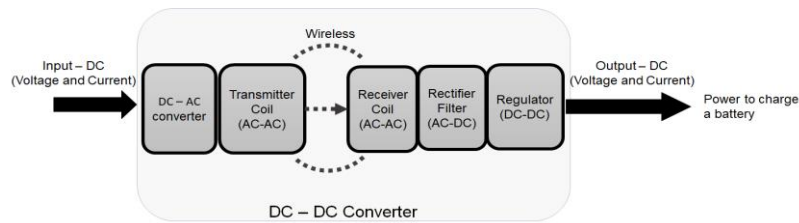
Fig. 2. A block-level representation of a wireless power system that utilizes Near Field Magnetic Coupling (NFMC).

The choice of system depends on the use-case. For example, a highly coupled Inductive system where-in both the charger and device are not moving and the charger is placed at a single location of maximum coupling, may have a relatively simplistic coil design, and the design complexity may be on the converter circuits on the charger and receiver side. On the other hand, a system where positional flexibility of the device may be required. The complexity of such a system will result in significant design challenges not only on the converter circuits and their control, but also in the coil design.

The focus of this work will be on the charger (transmitter), with special focus on the coil and the coil-array design. The charger system is expected to provide power to devices that are proprietary as well as some devices that employ Qi [3] receivers, for example Android or iOS based smartphones.

It is important to recognize that multiple variables exist in the design process and there doesn't exist a way to simulate with high accuracy to obtain a final design. Instead, an analysis-simulation-prototyping-measurements based iterative steps are taken. In fact, even after a coil-array is designed, various system adjustments based on thermal issues, component cost and availability, EMI and Foreign Objects, should be expected when packaging for a final deployment. However, that detail is beyond the scope of this publication.

There are two fundamental limitations that face current systems in production. The first is the need to have the device receiving wireless power to be positioned directly above the transmitter coil in a nearly fixed position (With little xy spatial flexibility). The second limitation is the constraints on the z-distance between the charger and receiver.

In this part of a two-part publication, we will address the first challenge, i.e. the design of the transmitter coil system.

Section II will include introductory discussion of inductive wireless power systems and the design challenge for this work.

Section III will discuss the design process followed to develop the coil-array, followed by some concluding remarks.

2. Resonant/Inductive WPT Systems

2.1. Introduction.

As shown in Fig. 1, every wireless power system is a DC-to-DC converter, which can be further expanded for a NFMC system as shown in Fig. 2.

Both Magnetic Induction (MI) and Magnetic Resonance (MR), use the same physical principles, wherein a time-varying current through a coil (Transmitter or Primary) induces a Voltage in another coil (Receiver or Secondary) via the transformer action and both can be represented by Fig. 3. The difference is that MR systems utilize techniques to maintain operation closer to the resonance frequency of the system. Most commercial systems employed today operate in a quasi-MI-quasi-MR mode in that they are not perfectly resonant.

For example, in Qi systems certified by the Wireless Power Consortium (WPC), the devices are typically tuned at 100 kHz, and the operating frequency can be between 100 kHz and 205 kHz [3]. While suppliers and system designers use several techniques to control power (e.g. Duty Cycle, phase, dynamic selection between a half-bridge and a full-bridge), one technique is to vary the frequency of operation. For a description of how this can be done, refer to Fig. 3.

) coil, R (TX) is the intrinsic AC resistance of the TX coil, C1 is a tuning capacitor added to compensate for the reactance of the TX coil. Rs is the source resistance and the Voltage (Vs) the AC Voltage source. The L(RX), R(RX) and C2 denote the corresponding components on the Receiver (RX) side of the Wireless power system. The Z(Load) is the load seen by the system. It is typically variable and depends on the battery charge and the related Battery Management System (BMS). The impedance as seen by the Voltage source is given by Eqn. (1) below:

$$Z_{input} = Rs + R(Tx) + \left(\frac{1}{j\omega C1}\right) + \left(j\omega L(Tx)\right) + \frac{\omega^2 \kappa^2 L(Tx)L(Rx)}{j\omega L(Rx) + \left(\frac{1}{j\omega C2}\right) + R(Rx) + Z(Load)}$$

(1)

Assuming a constant voltage source, for a given system design and a given Z(load) value, the only variable for power control is ω, the frequency of operation. A frequency closer to the resonance of the TX coil increases the current in the TX coil, which in-turn increases the time-varying magnetic field strength that the RX coil couples to, which in-turn increases the voltage induced in the RX coil. Therefore, a system such as this operates close to purely inductive (for low power levels) and purely resonant (for higher power levels.
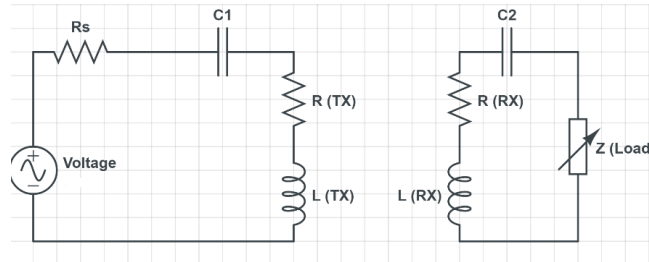

Fig. 3. A simpified and generalized system implementation of a wireless power system. The TX side is typically series-tuned as shown. The RX side could be series tuned (As shown) or parallel-tuned or a series/parallel combination. The tuning topology is a function of the system design and depends on the load impedance range, coupling and frequency of operation).

In addition to the above, there are other design considerations for any system. Some examples are the following:

Change of inductance parameters in the presence of the certain materials. For example, a receiver coil can change the inductance of the transmitter coil (and vice-versa), and this could alter the resonance frequency of the system. Therefore, a resonant system may only be useful for a system where the coupling is low.

- Change of circuit parameters (e.g. the magnetic properties of ferrite materials) at high fields or at high temperatures.

2.2. Target System

The objective of this work was to design a wireless transmitter system for industrial system applications that would exhibit the following characteristics:

- Compatibility with Consumer portable devices
- Spatial flexibility along x-axis (> 10 cms) and y-axis (~ 4 cms).
- Z-range greater than 30 mm (ideally 35 – 40 mm)
- Delivered power > 2.5W
- Transmitter coil dimensions should be 8 cms or less.

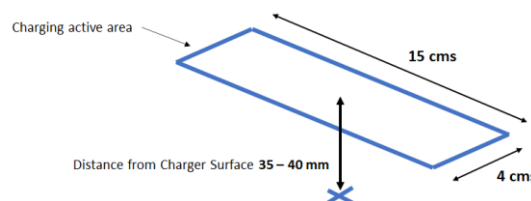Figure 4 and 5 illustrate the target system.
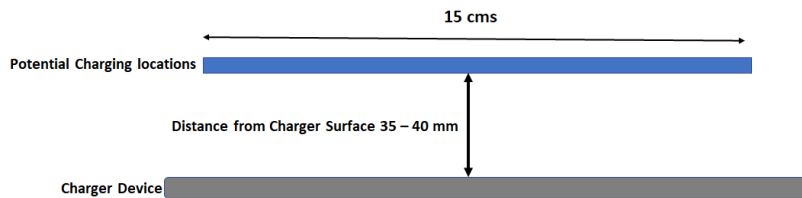

Fig. 4. The active charging area desired.

Fig. 5. A simpified Illustration of the target profile of the target system

For the technical problem, the size and specifications of the charger device (including coils, electronics) was flexible with a restriction on coil size (less than approximately 8 cm).

2.3. Background of Near Field Magnetic Coupling and Frequency Decision

The frequency is decided by specifications of size, range, EMI consideration, cost, heat, and installed infrastructure.

In NFMC Coupling, the transmitting coil creates a quasi-static Magnetic Field (H-field) region, called the Near Field (NF) Region, comprising H-field lines. Outside this region, the quasi-static H-field lines decay rapidly. If there is no receiver within the NF, no energy is lost by an *ideal* lossless source, unlike far-field where energy is lost via radiation even if there is no receiver. Realistically, energy is lost in the transmitting electronics, coil and coupling to surrounding devices.

There are three fundamental parameters that need to be met by any NFMC system to be efficient, safe, and reliable.

First, the distance between the transmitter and receiver should be less than the NF at the operating frequency. The extent of the near field is not exact and is typically defined as mentioned in Eqn. 2:

$$Near\ Field\ \approx \frac{\lambda}{2\pi} \tag{2}$$

Where λ is the wavelength at the operating frequency. This is a necessary but not a sufficient condition for useful transfer power.

Second, the Self-Resonance Frequency (SRF) of the transmitter and receiver antennas should be high. such that the current in the coils is quasi-static (i.e., there is negligible phase difference in current along the length of the coil filament). This is a a necessary condition in all applications but is not a sufficient in most. The SRF is a function of the environment and the materials around the antenna.

Third, the practical distance between the transmitter coil and the receiver coil is less than the size (e.g. diameter) of the transmitter coil. This is a necessary and sufficient condition for most applications.
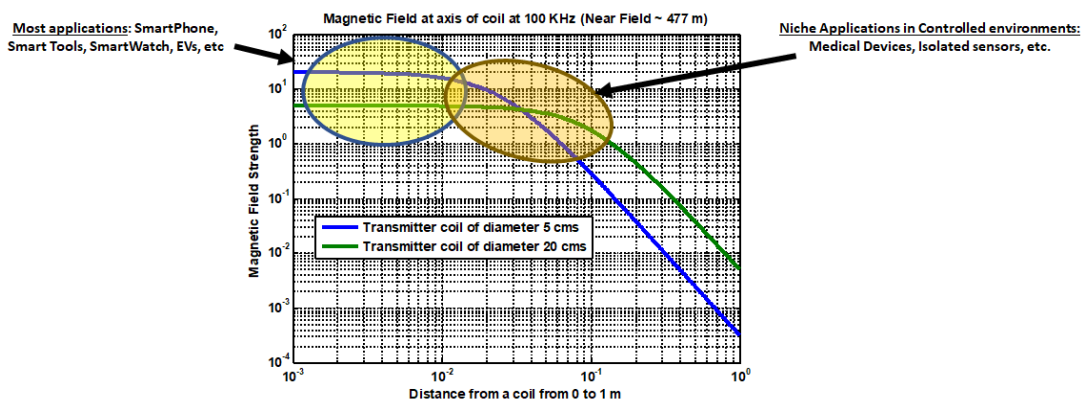

Fig. 6. This figure shows the decay of H-fields moving away from a coil and highlights the typical operating region of all systems in production (in yellow)

In Fig. 6, the magnetic field strengths of two exemplary coils are plotted. Realistic power transfer takes place in the region that lies within the "Flat" line; in other words, less than 10 cms for the coil of diameter 20 cms and less than 3 cms for the coil of diameter 5 cms. A rule of thumb is to keep the distance between coils less than the radius of the TX coil.

There could be some ultra-low power systems that could operate beyond the "flat-line" region. For consumer electronics (e.g. smartphones), all three factors are always true.

2.4. Design Process

Two parallel efforts were undertaken, the first was the design of the coil and the coil array, and the second was the design of the PCB board to drive the coils for measurements under power. Subsequently, tests were performed under power and modifications were made to the coil and coil-array as well as the PCB to maximize system performance.

This paper focusses on the design of the coil-system. In this work, an optimized approach to coil design is used – it uses a combination of empirical, analytical, and simulation methods.

3. Design of Coil Array

3.1. Introduction.

Several efforts to design a coil array have been undertaken in the past [9-10]. The WPC [3] has already certified litz-wire based and PCB-based arrays that can be used to charge mobile devices at distances less than 4 mm from the transmitter coil.

Important variables that need to be considered are shielding material, the gauge and number of strands in the litz-wire, number of layers in the coils and in the coil-array, overlap of the coils, shape of the coils, number of turns, and the outer and inner diameter of the coils. It is virtually impossible to optimize all the parameters analytically, and the process is a bit of an art form that is guided by analysis, simulations, fabrication, and testing.

For this design, it was decided to start with the design for a single coil that would then be replicated to create the array.

3.2. Analytical and Empirical

3.2.1. Calculation of the Magnetic Field Strength

As a starting point, an iPhone 8 device was used as a target receiver device. There were two reasons for this. First, it was determined that the iPhone 8 device was able to charge its battery when a sufficiently strong magnetic field was presented to it even without Qi-specific communication signals. The second reason was that using a standard and certified receiver product that is representative of most receiver systems allowed the focus to be on just the transmitter side of the system.

The well-known analytic formula based on Faraday's law of Electromagnetic Induction that can be applied over an area with uniform Magnetic field, H is given by Eqn. 3.

$$V_{Rx-induced} = \omega\mu A_{eff}H_{inc} \tag{3}$$

In the above equation, ω is the angular frequency of operation (=2πf), μ is the permeability of free space, A_{Eff} is the effective area of the receiver and H_{inc} is the magnetic field strength at the receiver coil. An assumption is that the H_{inc} is uniform across the effective area of the receiver coil.

The effective area, A_{Eff}, of the receiver was calculated to be 0.115 m^2. The following steps were done to obtain $V_{Rx\_induced}$.

Step-1: Place the device at 50 mm distance. 50mm was used for this (instead of the target) to add some buffer.

Step-2: Drive the TX coil with an AC power signal at the designated frequency (250 KHz and 300 kHz)

Step-3: Using a Qi-sniffer (from Avid technologies), obtain the power received by the device.

Step-4: Using a current probe (TCP0020), measure the current in the TX coil, I_{TX}.

Step-5: Replace the device with another device where the RX coil leads are disconnected from the device and connected to an oscilloscope to measure voltage across the RX coil.

Based on the above test and Eqn. 3, we are able to empirically determine the H_{inc} for various power levels.

It should be noted that it is being assumed that the H-field strength is uniform across the receiver coil.

Table 1 below shows the computed B field values from the induced voltage and power the power measurements. This target B-field values provides a starting point for the coil design process

Table 1: Computed B Field Values from the induced Voltage and Power Measurements. This B-Field Values is a starting point for the Coil Design Process

Power into Phone, W (measured)	Induced Voltage (measured)	Computed B (µT)
0.6	75	346.29
2.05	112	517.13
2.65	131	604.85
3.8	163	752.6
6.2	202	932.67

3.2.2 Determined Coil Topology (Turns, Layer, Size)

Eqn. 4 was used to estimate a starting value for the number of turns. The multi-loop is used to represent an N-turn coil with an average radius of "r".

$$H = \frac{\mu_0 N I r^2}{2(x^2 + r^2)^{3/2}} \tag{4}$$

The "H" is the magnetic field strength along the axis at a distance x from the coil plane where the coil is carrying a current I.

The following assumptions are made:

1. The H field scales linearly with the number of turns, assuming the turns are superposed

2. The radius of the n-turn loops is the average radius of the physical spiral coil being considered.

3. A current of approximately 7.5A was used. This is the rms current and is based on the current capability of the converter electronics (Imax < 9A rms).
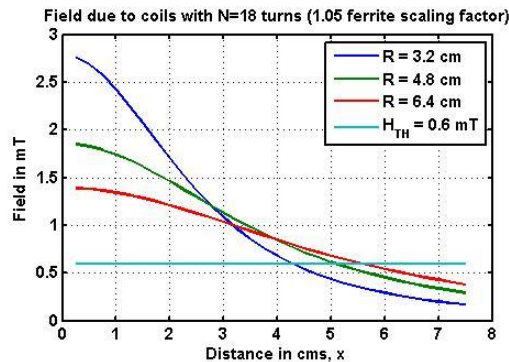

Fig. 7: Use "The plot of the H-field strength along the axis of an 18-turn coil with a certain average radius. The H-field strength needs to stay above the threshold at the required distance of 50mm (with buffer). The goal of the finished product is to charge through a 35mm – 40 mm distance.

Based on the figure, a good starting point for prototyping is to choose a coil of approximately 18 Turns and average radius between 32 mm and 48 mm, in order to generate a sufficient magnetic field strength. This data coupled with an outer dimension (diameter) of 80 mm creates the initial coil design.

3.3. Coil Fabrication and Characterization

For coils, using correct wire type and gauge is important. It has a direct impact on efficiency, thickness and even coupling. For frequencies less than 1 MHz, Litz wire is the preferred choice for transmitter coils for its low AC Resistance (ACR). The key selection criteria should be based on ACR (for low losses) at the operating frequency, number of strands (for overall low resistance), and the diameter (to keep overall coil thickness within desired limits). These criteria can be filtered to yield two key parameters:

1. Number of strands (Ns)

2. Gauge of each strand (G)

Eight coils were built and evaluated (See Table II). The 2 layer coils are designated as 2L.

Table 2: Measured Physical and Electrical Parameters of Fabricated Test Coils. The Electrical Parameters
(Inductance, AC Resistance are at 250 KHz)

Coil	Top.	Litz Type	Thick. (mm)	ID, OD (mm)	Ind. (µH)	AC Res.
C1	2L-21T	175/40	3.24	48, 82	65.9	0.36
C2	2L-18T	175/40	3.24	50, 82	50.1	0.26
C3	1L-10T	175/40	3.24	38, 69	12.8	0.074
C4	2L-21T	120/40	N/A	48, 80	62.1	0.28
C5	2L-21T	100/40	N/A	53, 80	67.1	0.35
C6	2L-22T	105/42	2.2	57, 81	92.2	0.43
C7	2L-22T	105/40	2.75	48, 81	74.5	0.38
C8	2L-22T	119/41	2.38	52, 81	82.6	0.39
C9	2L-20T	175/40	3.24	38, 69	43.5	0.23

Small-signal measurements in the context of coil characterization means that the measurements are taken under at low power (either with an LCR meter or Signal Generator and Oscilloscope) without any power conversion circuits. The coils are directly connected to the measurement instruments.

In order to accurately characterize coils for wireless power, coil-to-coil efficiency is ideal as it captures all key coil characteristics [10]. The equation for coil-coil efficiency is given by Eqn. 5

$$Coil - Coil\ efficiency = \frac{\kappa^2 Q_{Tx} Q_{Rx}}{(1 + \sqrt{1 + \kappa^2 Q_{Tx} Q_{Rx}})^2} \tag{5}$$

Where k is the coupling between a Transmitter coil (TX) and a receiver (RX) coil. QTx and QRx are the Quality factors of the TX and RX, respectively, measured at the operating frequency.

In our design problem, for the RX coil, a test coil is utilized.

Coupling Measurements: Coupling can be measured using at least two well-known techniques. The first method uses a signal generator and an oscilloscope while the other uses just an LCR meter. For the second technique the formula in Eqn. 6 can be used.

$$k = \sqrt{1 - \frac{L_{Tx}^s}{L_{Tx}^o}} \tag{6}$$

Where k is the coupling, L^s_{TX} is the inductance of the TX coil measured when the RX coil is shorted, and the L^o_{TX} is the inductance of the TX coil measured when the RX coil is open circuited. The basic measurement set up is shown in Fig. 8.
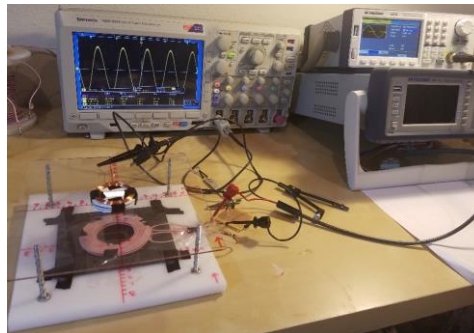

Fig. 8: Experimental Test Bench for Coupling Measurements..

Fig. 9 illustrates the calculated Coil-to-Coil efficiency (using equation 5) from measured data at 250 kHz.

Ferrite shields are an important part of the wireless power solution. The ferrite shield serves two purposes. First, it improves the coupling between the TX coil and the RX coil thereby improving the efficiency of the entire system. Second, it reduces the heating and potential damage to other components of the system due to the magnetic fields generated by the coils.
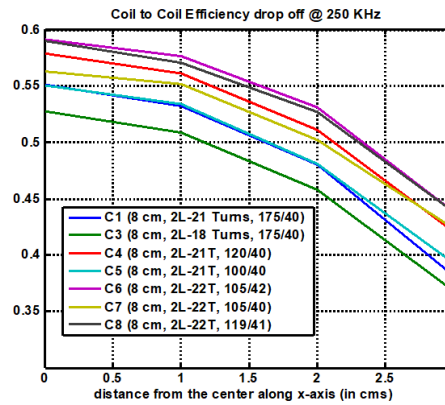
Fig. 9: Coil-to-Coil Efficiency computed using Eqn. 5 with measured Data

With the C6 coil as the baseline, multiple ferrites as shielding materials were evaluated (Fig. 9). Amongst these the EnE and the Laird performed very similarly. It was decided to proceed with the Laird material due to easy availability.

3.4. Coil Topology Selection

From the above discussion, Coil C6 appears to be the best choice. This leads to the next consideration, which is the design of a coil array. Some important considerations:

(1) The coupling with the RX for a given location of the device will change when the coils are stacked. For example, for a 2-layer array with a wire diameter, d illustrated in Fig. 11, the top layer coils are at the specification distance of D, while the bottom layer is at a specific distance of D plus the diameter, d, of the wire. In fact, if each coil is itself a 2-layer coil, then the distance of the lower layer coils will be D + 2d. In addition, the effect of the ferrite will be lesser for the top layer coils. Therefore, the litz-wire configuration becomes important.

(2) The stacked coils will make the solution thicker. The choice of ferrite dimension, coil topology (wire gauge, number of layers) will have a direct impact on this.

(3) Mutual coupling between the coils of the Coil-array is highly undesirable. It leads to a high impedance for the driver circuit making it difficult to drive a large current in the coils to create the necessary magnetic field strength. It also leads to unwanted I^2R losses. While the coil coupling can be reduced a bit by reducing the overlap of the coils, the major mitigation will be done using circuit techniques (future publication)
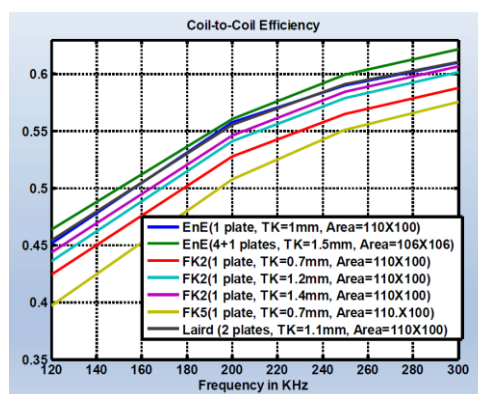

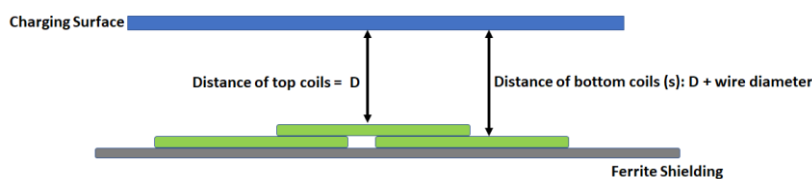Fig. 10: Coil-to-Coil Efficiency of a coil with various test ferrites

Fig. 11: Exemplary use-case illustrating the effect of layering for a coil-array

Thickness is a significant factor. For a single coil solution, C6 would be the leading choice; however, for a stacked coil solution, the coil closer to the ferrite would be about approximately 2.2 mm further away from the charging surface. This will reduce the coupling, k. Since the efficiency is proportional to k^2 (see Eqn. 5), it is desired to improve the k.

Therefore, it was decided to consider a single layer coil. The clear downside of a single layer coil is that the Q will be lower. For example, comparing C3 and C9 which have the same inner outer diameter and wire gauge (see Table II), the small signal $Q_{C9} \sim 297$ at 250 kHz, while $Q_{C3} \sim 272$. Using Eqn. 1, the coil-to-coil efficiency at maximum coupling position at distance of 38 mm is 80% and 79%, respectively. This difference is quite small.

There are several advantages of using a single-layer coil. The coil construction is simpler, and the coil material is lesser (leading to lower cost), the coupling between the coils when a coil-array is implemented will be higher (because of smaller d), the product package is thinner, and the reduced number of filaments will lead to lesser proximity effects. Further, a smaller inductance value will require a higher capacitance for tuning – this combination will have a greater tolerance to variations in capacitance values due to parasitic.

Therefore, the first modification from the initial coil designs was that a single layer coil would be chosen as a unit cell for the coil-array.

The second modification was based on the shape. Instead of a circular coil, a square coil was selected. The reason is that the square coil, because of its shape will provide marginally superior coupling (and performance) along the xy axis. There are tradeoffs that need to be kept in the design such as higher AC Resistance and lesser peak coupling. To enable easier manufacturing, square coils with rounded corners were selected. Both coils are illustrated in Fig. 12.

3.5. Coil Array Design

The strategy of implementing the coil array using the square coil design is illustrated in Fig. 13.

Depending on the availability of electronics, this array can be further scaled along the x-axis (along the length of the coil array) by adding more coils in the upper and lower layers
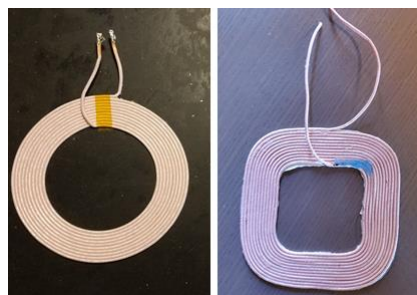

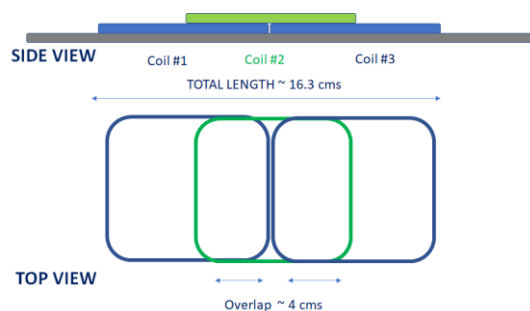Fig. 12: The one layer version of C9 (Circular) and its Square shape version.

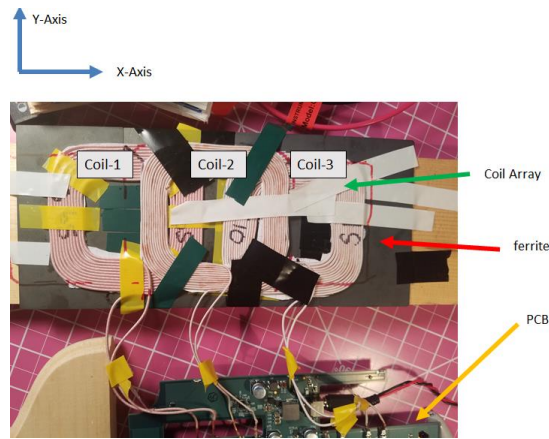Fig. 13 Initial Layout of the 3 coil array.

Fig. 14: Prototyped 3-coil array, with Coil-1 and Coil-3 separated.

4. Discussion and Conclusion

This paper describes the design process for a coil-system that can be used to provide wireless energy to a device at a distance greater than 30 mm and provides positional flexibility of position. The focus of the paper is to use a combination of analytical simulations, prototyping, characterization in an iterative loop to develop the design. A key contribution of this work is a scalable design process that can be adapted in size, frequency and power to suit wireless charging of other devices, for example mobile robots.

5. Acknowledgements

6. References

[1] N. Shinohara, "Trends in Wireless Power Transfer: WPT Technology for Energy Harvesting, Mllimeter-Wave/THz Rectennas, MIMO-WPT, and Advances in Near-Field WPT Applications," in IEEE Microwave Magazine, vol. 22, no. 1, pp. 46-59, Jan. 2021, doi: 10.1109/MMM.2020.3027935

[2] T. W. Ching and Y. S. Wong, "Review of wireless charging technologies for electric vehicles," 2013 5th International Conference on Power Electronics Systems and Applications(PESA), 2013, pp. 1-4, doi: 10.1109/PESA.2013.6828235.

[3] https://www.wirelesspowerconsortium.com/

[4] D. B. Ahire and V. J. Gond, "Wireless power transfer system for biomedical application: A review," 2017 International Conference on Trends in Electronics and Informatics (ICEI), 2017, pp. 135-140, doi: 10.1109/ICOEI.2017.8300903.

[5] https://www.wibotic.com/

[6] Derrick Wing Kwan Ng; Trung Q. Duong; Caijun Zhong; Robert Schober, "The Era of Wireless Information and Power Transfer," in Wireless Information and Power Transfer: Theory and Practice , Wiley, 2019, pp.1-16, doi: 10.1002/9781119476863.ch1

[7] N. Shinohara, "History and Innovation of Wireless Power Transfer via Microwaves," in IEEE Journal of Microwaves, vol. 1, no. 1, pp. 218-228, Jan. 2021, doi: 10.1109/JMW.2020.3030896.

[8] X. Lu, P. Wang, D. Niyato, D. I. Kim and Z. Han, "Wireless Charging Technologies: Fundamentals, Standards, and Network Applications," in IEEE Communications Surveys & Tutorials, vol. 18, no. 2, pp. 1413-1452, Secondquarter 2016, doi: 10.1109/COMST.2015.2499783.

[9] J. P. K. Sampath, A. Alphones and H. Shimasaki, "Coil design guidelines for high efficiency of wireless power transfer (WPT)," 2016 IEEE Region 10 Conference (TENCON), 2016, pp. 726-729, doi: 10.1109/TENCON.2016.7848098.

[10] R. Selvakumaran, W. Liu, B. H. Soong, L. Ming and S. Y. Loon, "Design of inductive coil for wireless power transfer," 2009 IEEE/ASME International Conference on Advanced Intelligent Mechatronics, 2009, pp. 584-589, doi: 10.1109/AIM.2009.5229950.

[11] R. Puers, et al., "A telemetry system for the detection of hip prosthesis loosening by vibration analysis," Sensors and Actuators A-Physical, vol. 85, pp. 42-47, Aug 2000